Acta Mechanica Sinica (2021) 37(4):662–678
https://doi.org/10.1007/s10409-020-01048-w

RESEARCH PAPER

A study on boundary integral equations for dynamic elastoplastic analysis for the plane problem by TD-BEM

Hongjun Li[1] · Weidong Lei[2] · Rui Chen[2] · Qiang Hu[3]

Received: 14 June 2020 / Revised: 17 November 2020 / Accepted: 17 December 2020 / Published online: 9 March 2021

Abstract
The equivalent stress fundamental solution for the elastoplastic dynamic plane strain problem is proposed to transform the virtual work in the third direction to the plane. Subsequently, based on Betti reciprocal theorem, by adopting the time dependent fundamental solutions in terms of displacement, traction and equivalent stress, the boundary integral equations for dynamic elastoplastic analysis for the plane strain problem are established. The establishment procedures for the displacement and the stress boundary integral equations, together with the stress equation at boundary points, are presented in details, while the standard discretization both in time and space under the frame of time domain boundary element method (TD-BEM) and the solution of the algebraic equations are also briefly stated. Two verification examples are presented from different viewpoints, for elastic and elastoplastic analysis, for 1-D and 2-D geometries, and for finite and infinite domains. The TD-BEM formulation for dynamic elastoplastic analysis is presented for the plane strain problem as an example, where the formulation is also applicable for the plane stress problem by properly transforming the elastic constants and adopting the corresponding fundamental solutions.

Keywords Time domain boundary element method · Dynamic elastoplastic analysis · Equivalent stress fundamental solution · Boundary integral equation

1 Introduction

It is well known that the general problem of the determination of the response of elastoplastic structures to dynamic loads can only be solved by numerical methods [1]. In the past several decades, with the drastic evolution of digital computers, the finite element method (FEM) has become the predominant numerical tool in dynamic elastoplastic analysis. The boundary element method (BEM) has played a secondary role, however in some cases, appeared to be a better choice than FEM due to the inherent advantages of the algorithm in BEM formulation [1–6].

There are three different BEM formulations for dynamic elastoplastic analysis, that is, the domain boundary element formulation (D-BEM) [7–9], the dual reciprocity boundary element formulation (DR-BEM) [9–12], and the time-domain boundary element formulation (TD-BEM) [13–16]. In both of the first and the second formulations, static fundamental solutions are employed, distinguished by the treatment of the inertial integral, where keeping the inertial integral in the characteristics equation generates D-BEM, while transforming the inertial integral into a boundary one generates DR-BEM. In the third formulation for dynamic elastoplastic analysis, TD-BEM, dynamic fundamental solutions are considered in the direct conventional BEM frame.

From the brief comparison among the aforementioned three BEM formulations for dynamic elastoplastic analysis, it can be seen that the boundary integral equations in the formulations, where the fundamental solutions are adopted, play the essential role. For this research topic, the readers could refer to the review works by Beskos et al. [1–3], the original TD-BEM formulation by Banerjee et al. [14,

Executive Editor: Xu Guo

✉ Weidong Lei
leiwd@hit.edu.cn

[1] Urban and Rural Construction Institute, Hebei Agricultural University, Baoding 071001, China

[2] School of Civil and Environmental Engineering, Harbin Institute of Technology (Shenzhen), Shenzhen 518055, China

[3] China Academy of Railway Sciences Corporation Limited, Beijing 100081, China

15], TD-BEM formulation coupling with other numerical methods by Soares [5], Soares et al. [17], Yu et al. [18] and Elleithy and Tanaka [19]. The TD-BEM formulation for dynamic elastoplastic problems was for the first time developed, with the whole numerical implementation and examples for plane problems in Ref. [14]. It is well known that, the plastic strain potentially exists in the third direction in dynamic elastoplastic analysis for the plane strain problem. Taking the stresses in the third direction in the plane strain problem into account, the virtual work in the third direction is accordingly produced. By contrast, in dynamic elastoplastic analysis for the plane stress problem, no plastic work in the third direction exists due to the assumption of none stress in the third direction, even the plastic strain potentially exists in the third direction. In the correct TD-BEM formulation for dynamic elastoplastic analysis for the plane strain problem, the virtual work in the third direction should be considered in the boundary integral equations. It is noted that the virtual work for the elastoplastic analysis for static plane strain problem was considered in Refs. [20, 21]. However, for the elastoplastic analysis for dynamic plane strain problem in Ref. [14], the virtual work, incorporated in $B_{ikj}\dot{\sigma}^0_{ik}$ in the second integral term in the displacement boundary integral equation in the literature, was not considered. Therefore, the boundary integral equations were only applicable for the dynamic plane stress problem. The same omission also existed in the other related Ref. [15], although the virtual work was incorporated in different expression due to different adopted notations.

In this paper, by establishing the equivalent stress fundamental solution, the virtual work in the third direction is considered in the boundary integral equations. The TD-BEM formulation for dynamic elastoplastic analysis is developed for the plane strain problem, and 1-dimensional and 2-dimensional numerical examples are used to validate the formulation. Due to the proper consideration of the virtual work in the third direction in the boundary integral equations, the TD-BEM formulation for dynamic elastoplastic analysis is also applicable for plane stress problems, by properly transforming the elastic constants and by adopting the corresponding fundamental solutions. In this paper, as an indispensable part of the standard TD-BEM formulation, the numerical discretization and the solution procedure are also briefly stated.

2 Establishment of the boundary integral equation

Before presenting the main text of the paper, two points should be pointed out. First, the TD-BEM formulation in this paper is presented for the plane strain problem without gravity. By replacing the fundamental solutions for the plane strain problem with those for the plane stress problem, also respectively replacing the Young modulus E and Poisson's ratio ν in the expression of the Lame constant λ with $E(1+2\nu)/(1+\nu)^2$ and $\nu/(1+\nu)$, and keeping the other Lame constant μ (shear modulus) unchanged, the TD-BEM formulation for the plane strain problem is transformed into TD-BEM formulation for the plane stress problem. Second, for the plane problem with constant body force, such as gravity, based on the TD-BEM formulation for the plane problem without body force, the additional boundary integral is needed.

The boundary integral equation for elastoplastic dynamics by the initial strain method can be constructed by following the similar procedure for inelastic statics and elastoplastic dynamics by the method of the initial stress method [20, 22]. Namely, based on Betti reciprocal theorem, by integrating over τ from instant 0 to t, the displacement boundary integral equation, Eq. (1), can be obtained, where the last term, the domain integral term, corresponds to the dissipation work in the plastic region

$$\begin{aligned} c_{ik}u_i(P,t) = &-\int_\Gamma\int_0^t p^*_{ik}(P,\tau;Q,t)u_k(Q,\tau)\mathrm{d}\tau\mathrm{d}\Gamma \\ &+\int_\Gamma\int_0^t u^*_{ik}(P,\tau;Q,t)p_k(Q,\tau)\mathrm{d}\tau\mathrm{d}\Gamma \\ &+\int_\Omega\int_0^t \overline{\sigma}^*_{ikl}(P,\tau;R,t)\varepsilon^p_{kl}(R,\tau)\mathrm{d}\tau\mathrm{d}\Omega. \end{aligned} \tag{1}$$

In the above equation, c_{ik} is the position coefficient, which was explained TD-BEM literatures, and could be found with ease for interested readers. The displacement and traction fundamental solutions in the equation are expressed in Eqs. (2) and (3) [23] as:

$$\begin{aligned} u^*_{ik} = &\frac{1}{2\pi\rho c_s}[(E_{ik}L_s + F_{ik}L_s^{-1} + J_{ik}L_sN_s)H_s \\ &-\frac{c_s}{c_d}(F_{ik}L_d^{-1} + J_{ik}L_dN_d)H_d], \end{aligned} \tag{2}$$

$$p^*_{ik} = \frac{1}{2\pi\rho c_s}\left\{A_{ik}\left[rL_s^3H_s + L_s\frac{\partial H_s}{\partial(c_s\tau)}\right] + B_{ik}L_sN_sH_s + \frac{D_{ik}}{r^2}\left[r^3L_s^3H_s + L_sN_s\frac{\partial H_s}{\partial(c_s\tau)}\right] - \frac{c_s}{c_d}\left\{B_{ik}L_dN_dH_d + \frac{D_{ik}}{r^2}\left[r^3L_d^3H_d + L_dN_d\frac{\partial H_d}{\partial(c_d\tau)}\right]\right\}\right\}, \tag{3}$$

where the parameters are explained in Appendix A.

The equivalent stress fundamental solution $\overline{\sigma}^*_{ikl}$ is further determined in the following context. By recalling the theorem of elasticity, the stress fundamental solution σ^*_{ikl} represent the stress at k direction in the plane with the normal vector of n_l at field point Q at instant t, due to the unit impulse at i direction at source point P at instant τ. Therefore, for the same plane, the traction p^*_{ik} and the stress σ^*_{ikl} at field point Q are the same, which can be expressed as:

$$\sigma^*_{ikl}(P,\tau;Q,t) = \left[p^*_{ik}(P,\tau;Q,t)\right]_{n_w=\delta_{lw}}, \quad w = 1,\ 2. \tag{4}$$

The stress fundamental solution for plane stress problem can be expressed, as:

$$\sigma^*_{ikl} = \frac{1}{2\pi\rho c_s}\left\{A_{ikl}\left[rL_s^3H_s + L_s\frac{\partial H_s}{\partial(c_s\tau)}\right] + B_{ikl}L_sN_sH_s + \frac{D_{ikl}}{r^2}\left[r^3L_s^3H_s + L_sN_s\frac{\partial H_s}{\partial(c_s\tau)}\right] - \frac{c_s}{c_d}\left\{B_{ikl}L_dN_dH_d + \frac{D_{ikl}}{r^2}\left[r^3L_d^3H_d + L_dN_d\frac{\partial H_d}{\partial(c_d\tau)}\right]\right\}\right\}. \tag{5}$$

By comparing Eq. (5) with Eq. (3), it is found that σ^*_{ikl} is expressed in the same format with p^*_{ik}, by replacing the subscript ik with ikl. The parameters in Eq. (5) are also explained in Appendix A.

However, the equivalent stress fundamental solution is different from the stress fundamental solution. For the plane strain problem, the stress fundamental solution for the third direction is not zero, which could be expressed as:

$$\begin{aligned}\sigma^*_{i33} &= \nu\sigma^*_{imm}\\ &= \frac{1}{2\pi\rho c_s}\left\{\Delta A_{imm}\left[rL_s^3H_s + L_s\frac{\partial H_s}{\partial(c_s\tau)}\right] + \frac{\Delta D_{imm}}{r^2}\left[r^3L_s^3H_s + L_sN_s\frac{\partial H_s}{\partial(c_s\tau)}\right] - \frac{c_s}{c_d}\frac{\Delta D_{imm}}{r^2}\left[r^3L_d^3H_d + L_dN_d\frac{\partial H_d}{\partial(c_s\tau)}\right]\right\},\end{aligned} \tag{6}$$

where

$$\Delta A_{imm} = -\Delta D_{imm} = 2\nu\mu(2\varphi+1)r_{,i} \quad m = 1,2. \tag{7}$$

According to Law of volume elasticity, one has

$$e^p = \varepsilon^p_{11} + \varepsilon^p_{22} + \varepsilon^p_{33} = 0, \tag{8}$$

i.e.

$$\varepsilon^p_{33} = -\left(\varepsilon^p_{11} + \varepsilon^p_{22}\right) = -\varepsilon^p_{kl}\delta_{kl}. \tag{9}$$

It is obvious that, even for the plane strain problem, the plastic strain at the third direction might not be zero either. Therefore, the stress at the third direction potentially produces the virtual work, whose effects should be considered in the boundary integral equations in TD-BEM formulation for plane strain problem. In order to equivalently transform the virtual work at the third direction into the plane, one has

$$w_3 = -\sigma^*_{i33}\varepsilon^p_{kl}\delta_{kl}. \tag{10}$$

Therefore, the last integrand in boundary integral equation Eq. (1) is expressed as

$$\sigma^*_{ikl}\varepsilon^p_{kl} + \sigma^*_{i33}\varepsilon^p_{33} = \sigma^*_{ikl}\varepsilon^p_{kl} - \sigma^*_{i33}\varepsilon^p_{kl}\delta_{kl} = (\sigma^*_{ikl} - \sigma^*_{i33}\delta_{kl})\varepsilon^p_{kl}. \tag{11}$$

One can express the equivalent stress fundamental solution for the plane strain problem as follows:

$$\overline{\sigma}^*_{ikl} = \sigma^*_{ikl} - \sigma^*_{i33}\delta_{kl}. \tag{12}$$

Then, the equivalent stress fundamental solution for the plane strain problem can be obtained as:

$$\overline{\sigma}^*_{ikl} = \frac{1}{2\pi\rho c_s}\left\{\overline{A}_{ikl}\left[rL_s^3H_s + L_s\frac{\partial H_s}{\partial(c_s\tau)}\right] + \overline{B}_{ikl}L_sN_sH_s + \frac{\overline{D}_{ikl}}{r^2}\left[r^3L_s^3H_s + L_sN_s\frac{\partial H_s}{\partial(c_s\tau)}\right] - \frac{c_s}{c_d}\left\{\overline{B}_{ikl}L_dN_dH_d + \frac{\overline{D}_{ikl}}{r^2}\left[r^3L_d^3H_d + L_dN_d\frac{\partial H_d}{\partial(c_d\tau)}\right]\right\}\right\}, \tag{13}$$

where the parameters are also explained in Appendix A.

Therefore, the virtual work is eliminated from the equivalent stress fundamental solution. And the equivalent stress integral term in the boundary integral equation is expressed in Eq. (14) as:

$$\begin{aligned}&\int_\Omega\int_0^t \overline{\sigma}^*_{ikl}\varepsilon^p_{kl}\mathrm{d}\tau\mathrm{d}\Omega\\ &= \frac{1}{2\pi\rho c_s}\int_\Omega\left[(\overline{A}_{ikl} + \overline{D}_{ikl})\overline{\int_0^t rL_s^3\varepsilon^p_{kl}H_s\mathrm{d}\tau} + \overline{B}_{ikl}\int_0^t L_sN_s\varepsilon^p_{kl}H_s\mathrm{d}\tau\right.\\ &\left. -\frac{c_s}{c_d}\left(\overline{B}_{ikl}\int_0^t L_dN_d\varepsilon^p_{kl}H_d\mathrm{d}\tau + \overline{D}_{ikl}\overline{\int_0^t rL_d^3\varepsilon^p_{kl}H_d\mathrm{d}\tau}\right)\right]\mathrm{d}\Omega,\end{aligned} \tag{14}$$

where the symbol "$\overline{\ \ \ }$" represents the finite part of an integral, for which one can refer Ref. [24].

3 Establishment of the stress boundary integral equation at interior points

For elastoplastic dynamics, the unknowns cannot be independently solved by the displacement boundary integral equation. In the process of solving the unknowns, the stress boundary integral equation at interior points is a must, which is based on the physical and the geometric equations.

The physical equation is

$$\sigma_{ij}(P,t) = \sigma^{e}_{ij}(P,t) - \sigma^{p}_{ij}(P,t), \tag{15}$$

where the imaginary elastic stress and plastic stress, σ^{e}_{ij} and σ^{p}_{ij}, are expressed as:

$$\begin{cases} \sigma^{e}_{ij}(P,t) = \lambda\delta_{ij}\varepsilon_{mm}(P,t) + 2\mu\varepsilon_{ij}(P,t), \\ \sigma^{p}_{ij}(P,t) = \lambda\delta_{ij}\varepsilon^{p}_{mm}(P,t) + 2\mu\varepsilon^{p}_{ij}(P,t). \end{cases} \tag{16}$$

The differential relationship between the total stress and the total strain are expressed in the geometric equation as follows:

$$\varepsilon_{ij}(P,t) = \frac{1}{2}\left[u_{i,j}(P,t) + u_{j,i}(P,t)\right]. \tag{17}$$

Putting the displacement boundary integral equation at interior points into Eq. (17), and combining the physical equation and the geometric equation, the stress boundary integral equation at interior points can be obtained. The kernel functions in terms displacement, traction and strain influence coefficients, s^{*}_{ijk}, d^{*}_{ijk} and $\overline{\sigma}^{*}_{ijkl}$, are respectively expressed as:

$$\begin{cases} s^{*}_{ijk} = \lambda\delta_{ij}p^{*}_{mk,m} + \mu\left(p^{*}_{ik,j} + p^{*}_{jk,i}\right), \\ d^{*}_{ijk} = \lambda\delta_{ij}u^{*}_{mk,m} + \mu\left(u^{*}_{ik,j} + u^{*}_{jk,i}\right), \\ \overline{\sigma}^{*}_{ijkl} = \lambda\delta_{ij}\overline{\sigma}^{*}_{mkl,m} + \mu\left(\overline{\sigma}^{*}_{ikl,j} + \overline{\sigma}^{*}_{jkl,i}\right). \end{cases} \tag{18}$$

The kernel function in terms of strain influence coefficients, $\overline{\sigma}^{*}_{ijkl}$, could not be directly calculated by using the equation, $s^{*}_{ijk} = n_l\overline{\sigma}^{*}_{ijkl}$, additionally, $u_{i,j}(X(P),t)$ and $u_{j,i}(X(P),t)$ in the geometric equation stand for the derivatives with respect to the coordinate of the source point. It means that the newly emerged derivatives in the above equations are regarding with the coordinate of the source point. The stress boundary integral equation at interior points is expressed as:

$$\begin{aligned} \sigma_{ij}(P,t) = &-\int_{\Gamma}\int_{0}^{t} s^{*}_{ijk}(P,\tau;Q,t)u_k(Q,\tau)\mathrm{d}\tau\mathrm{d}\Gamma \\ &+\int_{\Gamma}\int_{0}^{t} d^{*}_{ijk}(P,\tau;Q,t)p_k(Q,\tau)\mathrm{d}\tau\mathrm{d}\Gamma \\ &+\int_{\Omega}\int_{0}^{t} \overline{\sigma}^{*}_{ijkl}(P,\tau;R,t)\varepsilon^{p}_{kl}(R,\tau)\mathrm{d}\tau\mathrm{d}\Omega - \sigma^{p}_{ij}(P,t)xf^{P}_{ij}. \end{aligned} \tag{19}$$

The notations in Eq. (19), together with the coefficients, which are solely relevant with the spatial coordinate, are listed in Appendix B, while the others are listed in Appendix A.

It needs to specially point out that both the displacement integral equation and the stress boundary integral equation are applicable in both finite and infinite problems. For infinite problem, two additional integrals, $\lim_{r\to\infty}\int_{\Gamma_r}\int_0^t u^{*}_{ik}p_k\mathrm{d}\tau\mathrm{d}\Gamma$ and $\lim_{r\to\infty}\int_{\Gamma_r}\int_0^t p^{*}_{ik}u_k\mathrm{d}\tau\mathrm{d}\Gamma$, should be included in the boundary integral equations, where r stands for the radius of the virtual out boundary of a big circle, Γ_r, surrounding the internal boundary Γ. When ρ approaches the infinity, $r\to\infty$, the finite problem turns to the infinite problem. However, the two integral terms in dynamics are different from those in statics. In a dynamic problem, only in the case where $M_w = c_w(t-\tau) - r \geq 0$, i.e., $H(M_w) = 1$, the two integral terms are not zero. In the case of $r\to\infty$, one has $H(M_w) = 0$, meaning that the two integral terms naturally disappear in a dynamic problem.

The wave front of an impulse, that initiates at any instant within the analysis duration [0, t], cannot reach the infinity before t instant. It means that the impulse has none impacts on, such as the displacement, velocity, traction, stress and strain, for the infinity during the analysis duration. In this sense, the phenomenon is reasonably explained. Moreover, the phenomenon could also be illustrated from the viewpoint of the difference between the treatment mechanisms for statics and dynamics. In statics, only if the internal force acts in an infinite elastic body, the resultant force on the virtual outer boundary of a big circle Γr is always equal in amount and opposed in direction to the resultant internal force, where the effects from the virtual outer boundary could not be neglected. By contrast, in dynamics, the impulse initiated at any instant in the finite analysis duration, definitely cannot reach the infinity, the infinite outer boundary has none influence on the problem.

By comparing the boundary integral equations in Refs. [1, 3, 13] and in this paper, it can be seen that an additional domain integral is included in elastoplastic dynamics. The domain integral accounts for the energy dissipation due to plasticity. By comparing with the boundary integral equations for both elastostatics in Refs. [25, 26] and elastoplastic dynamics in this paper, it can be seen that time dependent transient fundamental solutions are adopted.

4 Stress equation at boundary points

According to the idea of the standard dynamic TD-BEM formulation, source point P is supposed to traverse every node in the expected elastoplastic domain. In some cases, the internal element in the elastoplastic domain is so close to the boundary, that some nodes of the internal elements would be coincident

with the boundary nodes. If source point P goes through the coincident node connecting the internal element in the elastoplastic domain and the boundary element, hyper singularity is encountered, where the singularity treatment for the other internal node is not applicable. In this scenario, the stress equation at boundary points is proposed to calculate the stress for the points on the boundary.

Supposing that the displacement, traction and plastic strain at the boundary points are given, the stress equation at boundary points is easy to be obtained by combining Hooke's law and the boundary condition. For the coincident node connecting the internal element in the elastoplastic domain and the boundary element, according to the general Hooke's law, one has:

$$\sigma_{ij} = \mu\left(u_{i,j} + u_{j,i}\right) + \lambda\delta_{ij}u_{m,m} - \sigma^p_{ij}, \tag{20}$$

where $\sigma^p_{ij} = 2\mu\varepsilon^p_{ij} + \lambda\delta_{ij}\epsilon^p_{mm}$.

The equation is written in matrix format as:

$$\boldsymbol{\sigma} = Cu' - \sigma^p, \tag{21}$$

where

$$\boldsymbol{\sigma} = \left(\sigma_{11}^{(m;e,Q)} \quad \sigma_{12}^{(m;e,Q)} \quad \sigma_{22}^{(m;e,Q)}\right)^{\mathrm{T}},$$

$$\boldsymbol{\sigma}^p = \left(\sigma_{11}^{p(m;e,Q)} \quad \sigma_{12}^{p(m;e,Q)} \quad \sigma_{22}^{p(m;e,Q)}\right)^{\mathrm{T}},$$

$$\boldsymbol{u}' = \left(u_{1,1}^{(m;e,Q)} \; u_{1,2}^{(m;e,Q)} \; u_{2,1}^{(m;e,Q)} \; u_{2,2}^{(m;e,Q)}\right)^{\mathrm{T}},$$

$$\boldsymbol{C} = \begin{bmatrix} 2\mu+\lambda & 0 & 0 & \lambda \\ 0 & \mu & \mu & 0 \\ \lambda & 0 & 0 & 2\mu+\lambda \end{bmatrix},$$

and m, e and Q in superscript $(m;e,Q)$ stand for the number of moment, element and node respectively.

However, in the above expression, Eq. (21), $\boldsymbol{\sigma}$, $\boldsymbol{\sigma}^{\mathrm{p}}$ and u' are unknown. In order to obtain u', the following two equations, Eqs. (22) and (23), are established based on the boundary condition.

The traction condition:

$$\mu\left(u_{i,j} + u_{j,i}\right)n_j + \lambda n_i u_{m,m} = p_i + \sigma^p_{ij}n_j \quad (i = 1, 2). \tag{22}$$

The displacement condition:

$$u_{i,j}\frac{\partial x_j}{\partial \xi} = \frac{\partial u_i}{\partial \xi} \quad (i = 1, 2). \tag{23}$$

On the boundary, $\partial u_i/\partial\xi$ and p_i can be expressed by the nodal displacement and traction in the corresponding boundary element as:

$$\begin{Bmatrix} \dfrac{\partial u_1^{(m;e,Q)}}{\partial \xi} \\ \dfrac{\partial u_2^{(m;e,Q)}}{\partial \xi} \end{Bmatrix} = \begin{bmatrix} \frac{\partial N_1}{\partial \xi} & 0 & \frac{\partial N_2}{\partial \xi} & 0 \\ 0 & \frac{\partial N_1}{\partial \xi} & 0 & \frac{\partial N_2}{\partial \xi} \end{bmatrix} \begin{Bmatrix} u_1^{(m;e,1)} \\ u_2^{(m;e,1)} \\ u_1^{(m;e,2)} \\ u_2^{(m;e,2)} \end{Bmatrix}, \tag{24}$$

$$\begin{Bmatrix} \dfrac{\partial x_1}{\partial \xi} \\ \dfrac{\partial x_2}{\partial \xi} \end{Bmatrix} = \begin{bmatrix} \frac{\partial N_1}{\partial \xi} & 0 & \frac{\partial N_2}{\partial \xi} & 0 \\ 0 & \frac{\partial N_1}{\partial \xi} & 0 & \frac{\partial N_2}{\partial \xi} \end{bmatrix} \begin{Bmatrix} x_1^{(e,1)} \\ x_2^{(e,1)} \\ x_1^{(e,2)} \\ x_2^{(e,2)} \end{Bmatrix}, \tag{25}$$

$$\begin{Bmatrix} p_1^{(m;e,Q)} \\ p_2^{(m;e,Q)} \end{Bmatrix} = \begin{bmatrix} N_1 & 0 & N_2 & 0 \\ 0 & N_1 & 0 & N_2 \end{bmatrix} \begin{Bmatrix} p_1^{(m;e,1)} \\ p_2^{(m;e,1)} \\ p_1^{(m;e,2)} \\ p_2^{(m;e,2)} \end{Bmatrix}. \tag{26}$$

Combining Eqs. (22) and (23), one has:

$$\boldsymbol{Bu'} = \boldsymbol{Np} + \boldsymbol{N'u} + \boldsymbol{V}\sigma^p. \tag{27}$$

That is

$$\boldsymbol{u'} = \boldsymbol{B}^{-1}\boldsymbol{Np} + \boldsymbol{B}^{-1}\boldsymbol{N'}u + \boldsymbol{B}^{-1}\boldsymbol{V}\boldsymbol{\sigma}^p, \tag{28}$$

where

$$\boldsymbol{B} = \begin{bmatrix} (2\mu+\lambda)n_1 & \mu n_2 & \mu n_2 & \lambda n_1 \\ \lambda n_2 & \mu n_1 & \mu n_1 & (2\mu+\lambda)n_2 \\ \frac{\partial x_1}{\partial \xi} & \frac{\partial x_2}{\partial \xi} & 0 & 0 \\ 0 & 0 & \frac{\partial x_1}{\partial \xi} & \frac{\partial x_2}{\partial \xi} \end{bmatrix},$$

$$\boldsymbol{N} = \begin{bmatrix} N_1 & 0 & N_2 & 0 \\ 0 & N_1 & 0 & N_2 \\ 0 & 0 & 0 & 0 \\ 0 & 0 & 0 & 0 \end{bmatrix}$$

$$\boldsymbol{N'} = \begin{bmatrix} 0 & 0 & 0 & 0 \\ 0 & 0 & 0 & 0 \\ \frac{\partial N_1}{\partial \xi} & 0 & \frac{\partial N_2}{\partial \xi} & 0 \\ 0 & \frac{\partial N_1}{\partial \xi} & 0 & \frac{\partial N_2}{\partial \xi} \end{bmatrix},$$

$$\boldsymbol{V} = \begin{bmatrix} n_1 & n_2 & 0 \\ 0 & n_1 & n_2 \\ 0 & 0 & 0 \\ 0 & 0 & 0 \end{bmatrix}.$$

Expressing $\boldsymbol{\sigma}^p$ by means of $\boldsymbol{\varepsilon}^p$, one has

$$\boldsymbol{\sigma}^p = \boldsymbol{C}^p \boldsymbol{\varepsilon}^p, \tag{29}$$

where $\boldsymbol{C}^p = \begin{bmatrix} 2\mu+\lambda & 0 & \lambda \\ 0 & 2\mu & 0 \\ \lambda & 0 & 2\mu+\lambda \end{bmatrix}$ and $\boldsymbol{\varepsilon}^p = \left(\varepsilon_{11}^{p(m;e,Q)} \ \varepsilon_{12}^{p(m;e,Q)} \ \varepsilon_{22}^{p(m;e,Q)} \right)^{\mathrm{T}}$.

Based on Eq. (29), putting Eq. (28) into Eq. (21), one has

$$\boldsymbol{\sigma} = -\boldsymbol{H}'^{(m;e)} \boldsymbol{u}^{(m;e,Q)} + \boldsymbol{G}'^{(m;e)} \boldsymbol{p}^{(m;e,Q)} + \boldsymbol{Q}'^{(m;e)} \boldsymbol{\varepsilon}^p, \tag{30}$$

where $\boldsymbol{G}'^{(m;e)} = \boldsymbol{C}\boldsymbol{B}^{-1}\boldsymbol{N}$, $\boldsymbol{H}'^{(m;e)} = -\boldsymbol{C}\boldsymbol{B}^{-1}\boldsymbol{N}\boldsymbol{Q}'$, $\boldsymbol{Q}'^{(m;e)} = (\boldsymbol{C}\boldsymbol{B}^{-1}\boldsymbol{V} - \boldsymbol{I})\boldsymbol{C}^p$.

The stress equation at boundary points is applicable for any point on the boundary. For the case where field point Q is located within the boundary element, it only needs to put the natural coordinate ξ of Q into the equation to calculate the stress. For the case where point Q is the node of the boundary element, the stress at point Q is calculated by averaging the stresses for the two adjacent boundary elements, connected by point Q. The stress equation at boundary points can be directly assembled together with the stress boundary integral equation at interior points. However, it should be noted that the shape function is used in the stress equation at boundary points. The shape function is an approximation, which might undermine the accuracy, by comparing with the stress boundary integral equation at interior points.

Upon the establishments of the boundary integral equations, the stress boundary integral equation at interior points, and the stress equation at boundary points, the basic equations for TD-BEM formulation for elastoplastic dynamics are established.

5 Numerical implementation and solution

Supposing that a unit impulse acts on a node in an element, in order to solve Eqs. (1) and (19) for an individual boundary element, the discretization both in time and space needs to be performed upon Eqs. (1) and (19). In the process of discretization, the time interval of the analysis duration $[0, t]$ is evenly divided into M time intervals, each with the same length of Δt, such that $t = M\Delta t$. In each time interval Δt, the linear time variation is conventionally assumed for the displacements $\boldsymbol{u}_k$ and the plastic strains ε_k^p, while the tractions $\boldsymbol{p}_k$ are assumed to be constant. The spatial discretization is performed on both the boundary and the part of the interior of the expected elastoplastic domain (3 nodded linear elements), where the linear spatial variation is assumed. After the time and spatial discretization, the boundary integral equations, Eqs. (1) and (19), are transformed into the discrete equations for each time and space element. Putting the discretized variables into the boundary integral equations, the displacement, traction and the plastic integral terms in the boundary integral equations, both on the boundary and in the expected elastoplastic domain, are expressed in the following discrete forms as:

$$\begin{aligned}
\int_\Gamma \int_0^t u_{ik}^* p_k \mathrm{d}\tau \mathrm{d}\Gamma &= \sum_{m=1}^{M} \sum_{e=1}^{N_e} \sum_{a=1}^{N_q} g_{ik}^{(m;e,a)} p_k^{(m;e,a)}, \\
\int_\Gamma \int_0^t p_{ik}^* u_k \mathrm{d}\tau \mathrm{d}\Gamma &= \sum_{m=0}^{M} \sum_{e=1}^{N_e} \sum_{a=1}^{N_q} \bar{h}_{ik}^{(m;e,a)} u_k^{(m;e,a)}, \\
\int_\Omega \int_0^t \bar{\sigma}_{ikl}^* \varepsilon_{kl}^p \mathrm{d}\tau \mathrm{d}\Omega &= \sum_{m=0}^{M} \sum_{f=1}^{N_f} \sum_{b=1}^{N_r} q_{ikl}^{(m;f,b)} \varepsilon_{kl}^{p(m;f,b)},
\end{aligned} \tag{31}$$

$$\begin{aligned}
\int_\Gamma \int_0^t d_{ijk}^* p_k \mathrm{d}\tau \mathrm{d}\Gamma &= \sum_{m=1}^{M} \sum_{e=1}^{N_e} \sum_{a=1}^{N_q} d_{ijk}^{(m;e,a)} p_k^{(m;e,a)}, \\
\int_\Gamma \int_0^t s_{ijk}^* u_k \mathrm{d}\tau \mathrm{d}\Gamma &= \sum_{m=0}^{M} \sum_{e=1}^{N_e} \sum_{a=1}^{N_q} s_{ijk}^{(m;e,a)} u_k^{(m;e,a)}, \\
\int_\Omega \int_0^t \bar{\sigma}_{ijkl}^* \varepsilon_{kl}^p \mathrm{d}\tau \mathrm{d}\Omega &= \sum_{m=0}^{M} \sum_{f=1}^{N_f} \sum_{b=1}^{N_r} \bar{f}_{ijkl}^{(m;f,b)} \varepsilon_{kl}^{p(m;f,b)}.
\end{aligned} \tag{32}$$

In Eqs. (31) and (32), N_e and N_f are amounts of the boundary elements and the domain elements, respectively. Due to the assumption of constant tractions in the time interval, the two influence coefficients, $g_{ik}^{(m;e,a)}$ and $d_{ijk}^{(m;e,a)}$, of the displacement of node a ($a=1, 2$) in boundary element e and the plastic strain of node b ($b=1, 2, 3$) in domain element f to the stress of source point P, are constant for every individual element. The other four coefficients, $\bar{h}_{ik}^{(m;e,a)}$, $s_{ijk}^{(m;e,a)}$, $q_{ikl}^{(m;f,b)}$ and $f_{ijkl}^{(m;f,b)}$, are expressed in the following equations (respectively corresponding to the influence of the displacement of node a ($a=1$, 2) in boundary element e to the displacement and stress of source point P, and the influence of the plastic strain of node b ($b=1$, 2, 3) in domain element f to the displacement and stress of source point P)

$$\bar{h}_{ik}^{(m;e,a)} = \begin{cases} \bar{h}_{ik}^{(m+1,1;e,a)} + \bar{h}_{ik}^{(m,2;e,a)}, & m = 1, 2, \cdots, M-1, \\ \bar{h}_{ik}^{(m,2;e,a)}, & m = M, \end{cases} \tag{33}$$

$$q_{ikl}^{(m;f,b)} = \begin{cases} q_{ikl}^{(m+1,1;f,b)} + q_{ikl}^{(m,2;f,b)}, & m = 1, 2, \cdots, M-1, \\ q_{ik}^{(m,2;f,b)}, & m = M, \end{cases} \tag{34}$$

$$s_{ijk}^{(m;e,a)} = \begin{cases} s_{ijk}^{(m+1,1;e,a)} + s_{ijk}^{(m,2;e,a)}, & m = 1, 2, \cdots, M-1, \\ s_{ijk}^{(m,2;e,a)} & m = M, \end{cases} \tag{35}$$

$$\bar{f}_{ijkl}^{(m;f,b)} = \begin{cases} \bar{f}_{ijkl}^{(m+1,1;f,b)} + f_{ijkl}^{(m,2;f,b)}, & m = 1, 2, \cdots, M-1, \\ \bar{f}_{ijkl}^{(m,2;f,b)}, & m = M. \end{cases} \tag{36}$$

After assemblage, the discrete 2-D time domain boundary integral equations are transformed into the following equations in matrix format:

$$\boldsymbol{h}^{MM}\boldsymbol{u}^{M} = \boldsymbol{g}^{MM}\boldsymbol{p}^{M} + \boldsymbol{q}^{MM}\boldsymbol{\varepsilon}^{pM} + \boldsymbol{a}^{M}, \tag{37}$$

$$\boldsymbol{\sigma}^{M} + \boldsymbol{s}^{MM}\boldsymbol{u}^{M} = \boldsymbol{d}^{MM}\boldsymbol{p}^{M} + \boldsymbol{f}^{MM}\boldsymbol{\varepsilon}^{pM} + \boldsymbol{b}^{M}, \tag{38}$$

where $\boldsymbol{a}^{M} = \sum_{m=0}^{M-1}\left(-\overline{\boldsymbol{h}}^{Mm}\boldsymbol{u}^{m} + \boldsymbol{g}^{Mm}\boldsymbol{p}^{m}\right) + \boldsymbol{q}^{Mm}\boldsymbol{\varepsilon}^{pm}$, $\boldsymbol{b}^{M} = \sum_{m=0}^{M-1}\left(-\boldsymbol{s}^{Mm}\boldsymbol{u}^{m} + \boldsymbol{d}^{Mm}\boldsymbol{p}^{m}\right) + \overline{\boldsymbol{f}}^{Mm}\boldsymbol{\varepsilon}^{pm}$.

As the unit impulse traverses all the boundary nodes, the overall time domain displacement boundary integral equation in matrix format Eq. (39) is obtained. As the unit impulse traverses all the domain nodes in the expected elastoplastic domain, the overall time domain stress boundary integral equation in matrix format Eq. (40) is obtained, in which the stress boundary integral equation at interior points and the stress equation at boundary points are incorporated

$$\boldsymbol{H}^{MM}\boldsymbol{u}^{M} = \boldsymbol{G}^{MM}\boldsymbol{p}^{M} + \boldsymbol{Q}^{MM}\boldsymbol{\varepsilon}^{pM} + \boldsymbol{A}^{M}, \tag{39}$$

$$\boldsymbol{\sigma}^{M} + \boldsymbol{S}^{MM}\boldsymbol{u}^{M} = \boldsymbol{D}^{MM}\boldsymbol{p}^{M} + \boldsymbol{F}^{MM}\boldsymbol{\varepsilon}^{pM} + \boldsymbol{B}^{M}, \tag{40}$$

where $\boldsymbol{A}^{M} = \sum_{m=0}^{M-1}\left(-\overline{\boldsymbol{H}}^{Mm}\boldsymbol{u}^{m} + \boldsymbol{G}^{Mm}\boldsymbol{p}^{m} + \boldsymbol{Q}^{Mm}\boldsymbol{\varepsilon}^{pm}\right)$, $\boldsymbol{B}^{M} = \sum_{m=0}^{M-1}\left(-\boldsymbol{S}^{Mm}\boldsymbol{u}^{m} + \boldsymbol{D}^{Mm}\boldsymbol{p}^{m} + \boldsymbol{F}^{Mm}\boldsymbol{\varepsilon}^{pm}\right)$, where the superscript "Mm" stands for the matrix when $t = M\Delta t$, $\tau = m\Delta t$. $\boldsymbol{H}, \boldsymbol{G}, \boldsymbol{S}, \boldsymbol{D}$ stand for the boundary influence matrices, and $\boldsymbol{Q}$ and $\boldsymbol{F}$ stand for domain influence matrices. $\boldsymbol{u}, \boldsymbol{p}$ and $\boldsymbol{\varepsilon}^{p}$ are vectors representing the displacement, traction, plastic strain, respectively.

Thus, the dynamic plasticity is described by the coupled system of the two integral equations, Eqs. (39) and (40). However, the integral equation set is undetermined, with the amount of unknowns more than that of equations. In order to solve the undetermined integral equation set, the additional relationship between plastic stress and plastic strain, i.e. the constitutive relation, needs to be supplemented. In this research, an elastoplastic material obeying the V. Mises isotropic hardening model is assumed, and the bilinear constitutive model is employed. When the node in the medium is under elastic state or unloading, by adopting the Hooke's law, one has:

$$\Delta\boldsymbol{\varepsilon}^{e} = \boldsymbol{D}_{e}\Delta\boldsymbol{\sigma}, \tag{41}$$

where $\Delta\boldsymbol{\varepsilon}^{e}$, $\Delta\boldsymbol{\sigma}$ and $\boldsymbol{D}_{e}$ respectively represent the elastic strain increment, stress increment of the node, and the flexibility matrix related to the elasticity modulus E, which is expressed as:

$$\boldsymbol{D}_{e} = \begin{bmatrix} \frac{1-\nu^2}{E} & 0 & -\frac{\nu(1+\nu)}{E} \\ 0 & \frac{(1+\mathrm{U})}{E} & 0 \\ -\frac{\nu(1+\nu)}{E} & 0 & \frac{1-\nu^2}{E} \end{bmatrix}. \tag{42}$$

When the node in the medium is under elastic–plastic state and loading, the total strain increment $\Delta\boldsymbol{\varepsilon}$ and the stress increment $\Delta\boldsymbol{\sigma}$ still obey the Hooke's law as:

$$\Delta\varepsilon = \boldsymbol{D}_{t}\Delta\boldsymbol{\sigma}, \tag{43}$$

where $\boldsymbol{D}_{t}$ represents the flexibility matrix related to the tangent modulus E_t, which is expressed as:

$$\boldsymbol{D}_{t} = \begin{bmatrix} \frac{1-\nu^2}{E_t} & 0 & -\frac{\nu(1+\nu)}{E_t} \\ 0 & \frac{(1+\nu)}{E_t} & 0 \\ -\frac{\nu(1+\nu)}{E_t} & 0 & \frac{1-\nu^2}{E_t} \end{bmatrix}. \tag{44}$$

Therefore the supplementary relationship between the plastic stress increment and the plastic strain increment is expressed as:

$$\Delta\varepsilon^{p} = \Delta\varepsilon - \Delta\varepsilon^{e} = \left(D_{t} - D_{e}\right)\Delta\sigma = D_{p}\Delta\sigma, \tag{45}$$

where $\boldsymbol{D}_{et}$ is defined as:

$$\boldsymbol{D}_{et} = \boldsymbol{D}_{t} - \boldsymbol{D}_{e} = \begin{bmatrix} \frac{1-\nu^2}{H'} & 0 & -\frac{\nu(1+\nu)}{H'} \\ 0 & \frac{(1+\nu)}{H'} & 0 \\ -\frac{\nu(1+\nu)}{H'} & 0 & \frac{1-\nu^2}{H'} \end{bmatrix}, \tag{46}$$

where $H' = \frac{EE_t}{E-E_t}$. $\boldsymbol{D}_{p}$ is a matrix with $\boldsymbol{D}_{et}$ and 3×3 zero matrix as diagonal submatrix, corresponding to yield point and non-yield point respectively.

So far, the dynamic plasticity is fully described by the coupled system of the two boundary integral equations, Eqs. (39) and (40), together with the constitutive relation, Eq. (45).

In order to solve the two boundary integral equations, besides the constitutive relation for determining the undetermined equation set, all of the elements in the influence matrices must be solved. In the process of the solution of the elements of the influence matrices, singularities must be treated. In this research, the elements in the influence matrices are divided into singular parts and non-singular parts to accordingly form the singular and non-singular submatrices, to be solved in different procedures. In order to treat the integral terms with hyper superficial singularities, the similar integral terms are coalesced to eliminate most of the singularities at first. For the remaining singularities, the treatment by calculating the Cauchy principle integral for the singular integrals was used to treat the singularities in other literatures [23, 27–29]. Besides the mathematical complexity, the method of rigid body displacement is an elastostatic concept, therefore, those singular treatments might not be applicable in nonlinear analysis both for elastoplastics and elastoplastic materials. Therefore, in this paper, Hadamard principle integral [24] is used to solve the singular integrals in discretization both in time and space, from the viewpoint

of dynamics, rather than the viewpoint of elastostatics. Interested readers could refer to literature [30] for the treatments to singularities in elastodynamics by using Hadamard principle integral. However, the full statement of the singularity treatment by using Hadamard principle integral is mathematically arduous, and will make the paper oversize, losing the focus of the paper and undermining the readability. The analytical treatments to the singularities by using Hadamard principle integral would be described in another independent paper. It is noted that the accurate evaluation of domain integrals is a big issue. There are two methods to evaluate the domain integrals, the internal cells-based method and the boundary-only method. The internal cells-based method is a direct method without special treatment, but the accuracy of integrals is dependent on the internal mesh. The boundary-only method can avoid the discretization of internal mesh and make good use of the advantages of BEM [31]. In our research, the internal cells-based method is adopted. When all of the integrals are obtained, all the elements in the influence matrices are solved.

The unknowns and the known elements of the nodal displacement and traction vectors are mixed in Eqs. (39) and (40). By separating the unknowns and the known elements and rearranging, Eqs. (39) and (40) are re-formulated as follows:

$$\boldsymbol{A}_1^{MM}\boldsymbol{x}^M = \boldsymbol{y}^M + \boldsymbol{Q}^{MM}\boldsymbol{\varepsilon}^{pM} + \boldsymbol{A}^M, \tag{47}$$

$$\boldsymbol{\sigma}^M = -\boldsymbol{A}_2^{MM}\boldsymbol{x}^M + \boldsymbol{z}^M + \boldsymbol{F}^{MM}\boldsymbol{\varepsilon}^{pM} + \boldsymbol{B}^M. \tag{48}$$

Equations (47)and (48) are rewritten as:

$$\boldsymbol{x}^M = \boldsymbol{R}^{MM}\boldsymbol{\varepsilon}^{pM} + \boldsymbol{Y}^M + \boldsymbol{K}^M, \tag{49}$$

$$\boldsymbol{\sigma}^M = \boldsymbol{T}^{MM}\boldsymbol{\varepsilon}^{pM} + \boldsymbol{Z}^M + \boldsymbol{L}^M, \tag{50}$$

where $\boldsymbol{R}^{MM} = \left(\boldsymbol{A}_1^{MM}\right)^{-1}\boldsymbol{Q}^{MM}$, $\boldsymbol{Y}^M = \left(\boldsymbol{A}_1^{MM}\right)^{-1}\boldsymbol{y}^M$, $\boldsymbol{K}^M = \left(\boldsymbol{A}_1^{MM}\right)^{-1}\boldsymbol{A}^M$, $\boldsymbol{T}^{MM} = \boldsymbol{F}^{MM} - \boldsymbol{A}_2^{MM}\boldsymbol{R}^{MM}$, $\boldsymbol{Z}^M = \boldsymbol{z}^M - \boldsymbol{A}_2^{MM}\boldsymbol{Y}^M$, $\boldsymbol{L}^M = \boldsymbol{B}^M - \boldsymbol{A}_2^{MM}\boldsymbol{K}^M$.

In the above algebra equations, all the matrices are solely dependent on the differential value of $(M-m)$. It means that two matrices, with different m value but with the same differential value of $(M-m)$, have the same element values. Therefore, if the response at the M-th time step is supposed to be solved, it only needs to obtain the corresponding matrices at the time step, with the maximum value of $(M-m)$, i.e., $(M-1)$. So, every new matrix for a time instant is saved for the forthcoming time step. The causality dramatically reduces the cost in the computation of matrices.

The stress at the M-th time step is expressed in incremental format as:

$$\boldsymbol{\sigma}^M = \boldsymbol{\sigma}^{M-1} + \Delta\boldsymbol{\sigma}^M,$$

where, $\Delta\boldsymbol{\sigma}^M = \boldsymbol{T}_p^{-1}\left(\Delta\boldsymbol{Z}^M + \Delta\boldsymbol{L}^M + \boldsymbol{Re}\right)$, $\boldsymbol{Re} = \boldsymbol{T}^{M,M-1}\boldsymbol{\varepsilon}^{p(M-1)} + \boldsymbol{Z}^{M-1} + \boldsymbol{L}^{M-1} - \boldsymbol{\sigma}^{M-1}$, $\boldsymbol{T}_p = \boldsymbol{I} - \boldsymbol{T}^{MM}\boldsymbol{D}_p$, and $\boldsymbol{I}$ is the identity matrix.

Analogously, the plastic strain at the M-th time step is obtained as:

$$\boldsymbol{\varepsilon}^{pM} = \boldsymbol{\varepsilon}^{p(M-1)} + \Delta\boldsymbol{\varepsilon}^{pM}, \tag{51}$$

where $\Delta\boldsymbol{\varepsilon}^{pM} = \boldsymbol{D}_p\Delta\boldsymbol{\sigma}^M$.

In order to treat the discontinuity of the slop of stress–strain curve at the transition period from elastic region to plastic region, a special treatment of sub-dividing the time intervals around the transition period is adopted. The amount of divisions in every time interval is dependent on the requirement of the evaluation accuracy, to guarantee that the calculated mechanical behavior in every sub-time-interval, in terms of the stress and strain increment, is close to the relationship between the stress and strain increment described by the constitutive law of the material.

So far, the computation in the M-th time step is finished, and the computation moves to the next time step, up to the last instant.

As all the unknowns on the boundary (the tractions and displacements) and in the expected elastoplastic domain (the plastic strain) are solved, the displacements of the interior points and the stresses of interior points in the non-plastic domain are solved by the following equations without any singularities:

$$\boldsymbol{u}_P^M = -\overline{\boldsymbol{H}}^{MM}\boldsymbol{u}^M + \boldsymbol{G}^{MM}\boldsymbol{p}^M + \boldsymbol{Q}^{MM}\boldsymbol{\varepsilon}^{pM} + \boldsymbol{A}^M, \tag{52}$$

$$\boldsymbol{\sigma}^M = -\boldsymbol{S}^{MM}\boldsymbol{u}^M + \boldsymbol{D}^{MM}\boldsymbol{p}^M + \overline{\boldsymbol{F}}^{MM}\boldsymbol{\varepsilon}^{pM} + \boldsymbol{B}^M, \tag{53}$$

where $\boldsymbol{A}^M = \sum_{m=0}^{M-1}\left(-\overline{\boldsymbol{H}}^{Mm}\boldsymbol{u}^m + \boldsymbol{G}^{Mm}\boldsymbol{p}^m + \boldsymbol{Q}^{Mm}\boldsymbol{\varepsilon}^{Pm}\right)$, $\boldsymbol{B}^M = \sum_{m=0}^{M-1}\left(-\boldsymbol{S}^{Mm}\boldsymbol{u}^m + \boldsymbol{D}^{Mm}\boldsymbol{p}^m + \boldsymbol{F}^{Mm}\boldsymbol{\varepsilon}^{pm}\right)$.

6 Verification

In order to verify the proposed 2-D TD-BEM formulation for dynamic elastoplastic analysis, two examples are chosen for verification, i.e., 1-D rod (shown in Fig. 1(a), where $a=2$ m) subjected to a Heaviside-type load, $p(t)=200$ MPa, $t\geq 0$ (shown in Fig. 1(c)), at the free side, and 2-D cavity in an infinite medium (shown in Fig. 1(b), where $r_0=1$ m) under the same Heaviside-type load as in the case of the 1-D rod on the cavity boundary.

It is noted that the elastoplastic response to transient dynamic loads can only be solved by numerical methods, without analytical solutions. Therefore, the results of the dynamic elastoplastic analysis from the TD-BEM

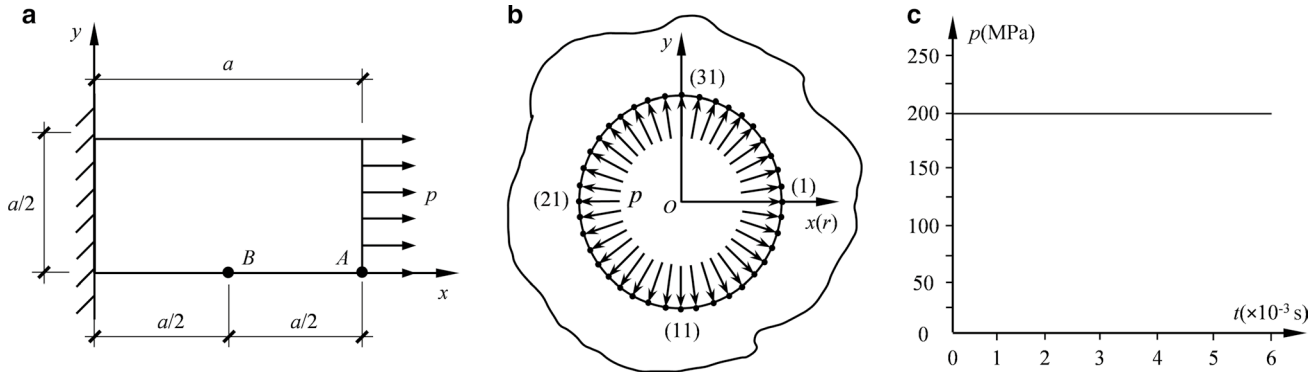

Fig. 1 Numerical examples and the load: **a** 1-D example, **b** 2-D example, and **c** Heaviside-type load

formulation in this paper are compared with those from the commonly used FEM program, Abaqus.

It is also noted that, if the third term in the boundary integral equations, Eq. (1), is excluded, the proposed TD-BEM formulation is degenerated from elastoplastic analysis to elastic analysis. It means that the degenerated TD-BEM formulation for elastic analysis is to some extent the bench mark of the formulation for elastoplastic analysis. Therefore, in order to enhance the convincingness of the verification for elastoplastic analysis, the degenerated TD-BEM formulation for elastic analysis is verified in advance, by comparing the elastic results from both FEM and the degenerated TD-BEM formulation for elastic analysis with the analytical solutions under the elastic conditions, which is more objective than the numerical solution.

Therefore, the proposed 2-D TD-BEM formulation for dynamic elastoplastic analysis is intensively validated from different viewpoints, for elastic and elastoplastic analysis, for 1-D and 2-D geometries, and for finite and infinite domains.

In order to determine the optimal time step, the TD-BEM results for different β values from the range of 0.5 to 1.0 are compared. The optimal time steps of 2×10^{-5} s, 1.5×10^{-5} s and 3.5×10^{-5} s are determined for 1-D elastic and elastoplastic examples, 2-D elastic example and 2-D elastoplastic example, respectively. It is noted that the accuracy of TD-BEM is sensitive to the time step [32]. Several researchers put forward improvement measures for elastodynamic TD-BEM, such as convolution quadrature method (CQM) [33, 34]. The stability of elastoplastic dynamic TD-BEM is worthy studying next.

6.1 Verification example of 1-D rod for elastic and elastoplastic analysis

6.1.1 1-D rod for elastic analysis

The classical 1-D rod under an axial Heaviside-type load was reported by some literatures for verification [26, 27, 35, 36]. In this paper, in order to clearly compare the modeling results by different TD-BEM formulations, it is also chosen to verify the degenerated TD-BEM formulation for dynamic elastic analysis, as shown in Fig. 1(a,b) for the geometry, in Fig. 1(c) for the load, $p(t)=200$ MPa, $t\geq0$. The transient elastic responses for two points A(2, 0) and B(1, 0) are chosen for the purpose of comparison.

The material parameters of the rod are: the elastic modulus $E=2.1\times10^{11}$ Pa, Poisson ratio $v=0$, mass density $\rho=7900$ kg/m^3. So, the velocity of the P wave is calculated as, $c_d=5156$ m/s. The boundary of the rod is evenly divided into 48 elements as shown in Fig. 2, and the time step 2×10^{-5} s is used in TD-BEM modeling. By contrast, in FEM program Abaqus, much finer mesh 0.005 m$\times$0.005 m is used to discretize the whole geometry of the problem, and the much shorter time step 5×10^{-7} s is employed.

The calculated transient displacements in two periods from the degenerated TD-BEM formulation for dynamic elastic analysis at two monitoring points A and B are shown in Fig. 3, in which, for the purpose of comparison, the displacements of the same two monitoring points both from the analytical solution [37] and FEM are also included.

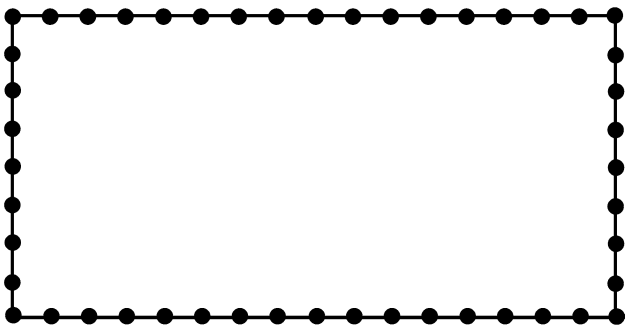

Fig. 2 Boundary discretization of 1-D rod

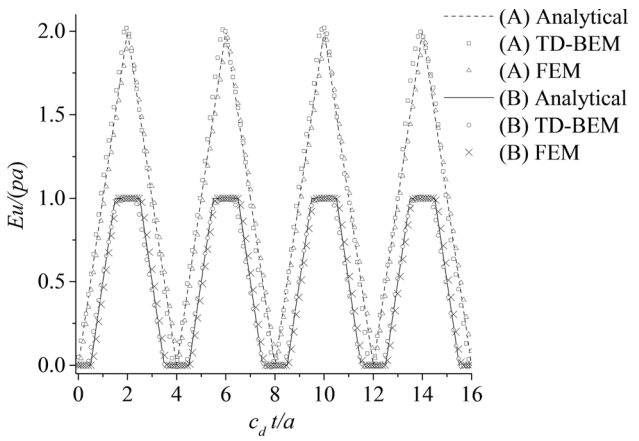

Fig. 3 Comparison between the results for displacement from TD-BEM, analytical and FEM for elastic analysis

From Fig. 3, it can be seen that both of the numerical results, from the degenerated TD-BEM and FEM, agree with the analytical solutions reasonably well.

6.1.2 1-D rod for elastoplastic analysis

The same 1-D rod in Fig. 1(a) subjected to the same Heaviside-type uniform load $p(t)=200$ MPa, $t\geq 0$ in Fig. 1(c) is used as the numerical example to verify the TD-BEM formulation for dynamic elastoplastic analysis. In order to ensure the occurrence of the plasticity in the medium, the tangent modulus of the material for bilinear constitutive model ($E_t=1\times10^{11}$ Pa) and the yield stress ($\sigma_s=2.1\times10^{8}$ Pa) are given to the mechanical properties of the material.

In TD-BEM model shown in Fig. 4, the whole geometry is discretized by 336 3-nodded boundary elements, with the mesh size 0.1 m × 0.1 m. And the time step 2×10^{-5} s is used. Therefore, 48 boundary nodes and 145 internal nods in the expected plastic region are generated. In FEM model, much finer mesh size 0.005 m × 0.005 m and the much shorter time step 5×10^{-7} s are employed again for the elastoplastic modeling.

The calculated elastoplastic transient displacements in two periods from TD-BEM formulation for dynamic elastoplastic analysis, together with those from FEM, at points A and B, are shown in Fig. 5. It can be seen that a good agreement between the TD-BEM and FEM has been achieved, with much more favorable mesh size and time step for FEM.

6.2 Verification example of 2-D cavity for elastic and elastoplastic analysis

6.2.1 2-D cavity for elastic analysis

Similar to the 1-D verification example, the 2-D example is used to verify the degenerated TD-BEM formulation for elastic analysis in advance as well. Suppose that the uniform Heaviside-type load, $p(t)=200$ MPa, $t\geq 0$, is suddenly applied on the boundary of the cylindrical cavity in an infinite medium, shown in Fig. 1(b,c). The material parameters of the medium are: the elastic modulus $E=2.1\times10^{11}$ Pa, Poisson ratio $v=0.3$, mass density $\rho=7900$ kg/m^3.

In BEM model, the internal boundary of the cylindrical cavity is divided into 40 linear boundary elements, with 40 linear boundary nodes, as shown in Fig. 1(b), and the time step 1.5×10^{-5} s is used. By contrast, the problem is modeled by a circular FEM model, with the outer artificial dynamic boundary, $r=100$ m, preventing from reflecting the outgoing wave. The whole FEM model is divided by quadrilateral elements. The mesh size 0.25 m × 0.25 m and the time step 1×10^{-6} s are used.

The calculated waves at $r=2$ m from the degenerated TD-BEM formulation for dynamic elastic analysis are shown in Fig. 6(a–c) in terms of the radial stress, the circumferential

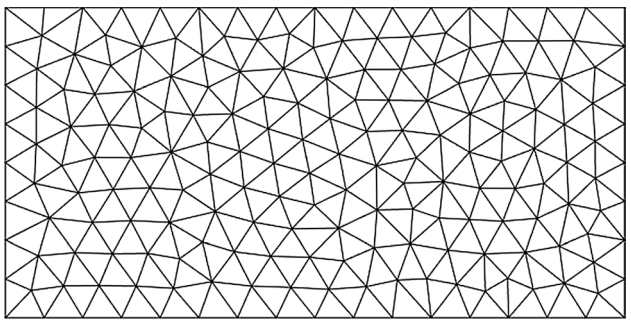

Fig. 4 Discretization of the boundary and suspicious plastic region of one-dimensional bar

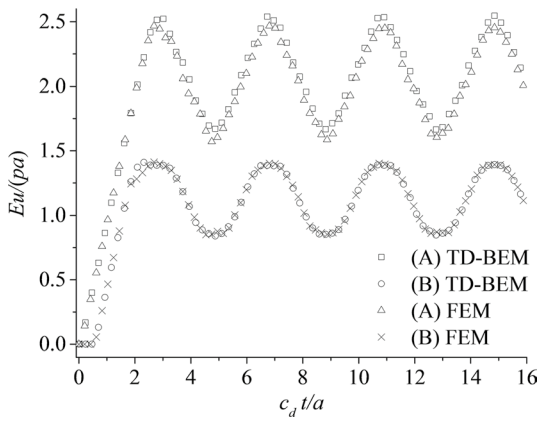

Fig. 5 Comparison between the results for displacement from TD-BEM and FEM for elastoplastic analysis

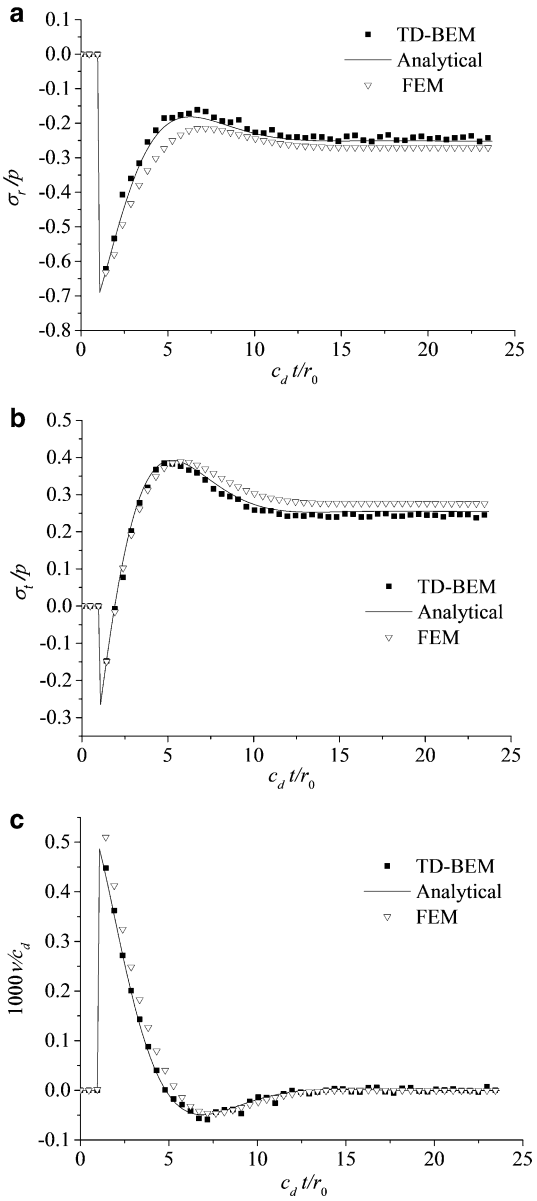

Fig. 6 Comparison between the results from TD-BEM, method of Characteristics and FEM for elastic analysis ($r=2$ m) for **a** radial stress, **b** circumferential stress, and **c** velocity.It should be noted that the stress and time are normalized, and the unit of the displacement is mm. Likewise, for the purpose of checking the computation stability for the degenerated TD-BEM formulation for dynamic elastic analysis, the corresponding calculated waves at a farther radial distance from the center of the cavity, $r=8$ m, are shown in Fig. 7(a–c)

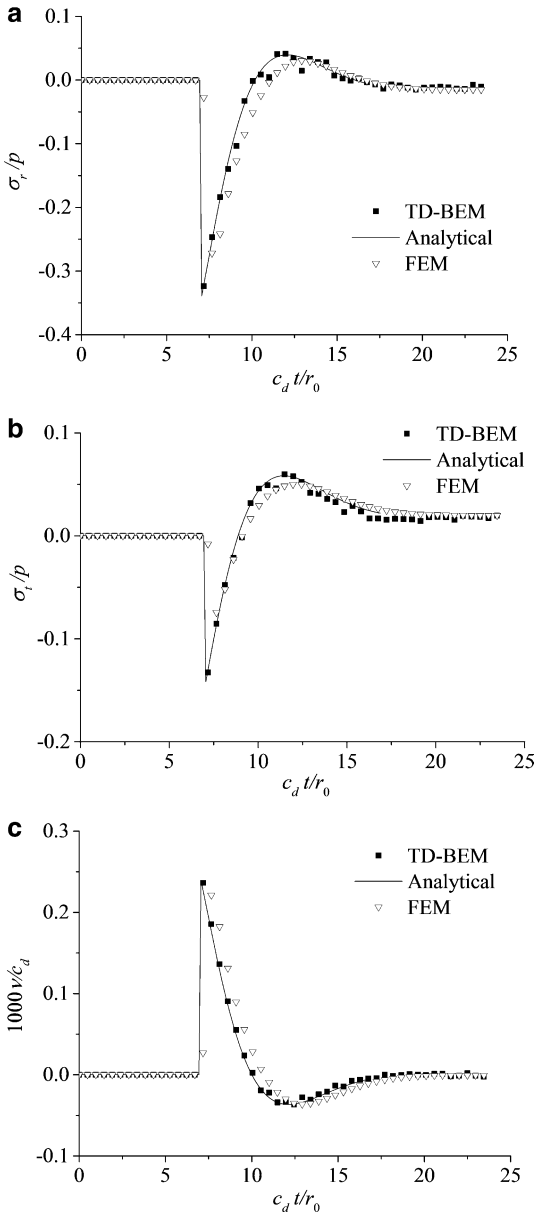

Fig. 7 Comparison between the results from TD-BEM, method of Characteristics and FEM for elastic analysis ($r=8$ m) for **a** radial stress, **b** circumferential stress, and **c** velocity

stress and the velocity, respectively, where the results from the method of characteristics, see reference by Chou and Koenig [38], and the results from FEM are also included. The velocity wave form TD-BEM formulation shown in Fig. 6(c) is calculated by using the following expression:

$$v = \frac{u_2 - u_1}{\Delta t}, \tag{54}$$

where u_1 and u_2 represent the displacement at the time node before and behind the calculating time node, and Δt represents the time step.

From Figs. 6 and 7, by comparing the objective analytical results and the numerical results, both from the degenerated TD-BEM formulation for dynamic elastic analysis and FEM, it can be seen that agreement between the numerical (TD-BEM and FEM) and the analytical results

is generally good for the points both close to and far away from the cavity boundary in the surrounding medium. By checking the agreements between the numerical (TD-BEM and FEM) and the objective analytical results at the turning point, where the wave arrive the peak value at the peak value occurrence instant, it can also be seen that the results from the degenerated TD-BEM formulation agree with the objective analytical solution, better than results from FEM do, probably due to the proper treatments on the singularities in TD-BEM formulation. Therefore, due to the inherent advantages in the algorithm in TD-BEM formulation, it is not strange that the performance of the degenerated TD-BEM formulation seems better than FEM for the infinite case, even under the unfavorable conditions of the mesh size and time step for the degenerated TD-BEM formulation for elastic analysis.

6.2.2 2-D cavity for elastoplastic analysis

The 2-D cavity subjected to the Heaviside-type, load $p(t)=200$ MPa, $t\geq 0$, in an infinite medium is also used to verify the whole TD-BEM formulation for dynamic elastoplastic analysis. In order to ensure the occurrence of the plasticity in the surrounding medium, the tangent modulus of the material for bilinear constitutive model ($E_t=1\times10^{11}$ Pa) and the yield stress ($\sigma_s=2.1\times10^{8}$ Pa) are given to the mechanical properties of the material.

In BEM model, the ring-shaped region defined by $1\text{ m}\leq r\leq 2$ m is chosen as the expected elastoplastic domain, where the internal boundary is divided into 41 1-D linear boundary elements, and the domain is divided into 443

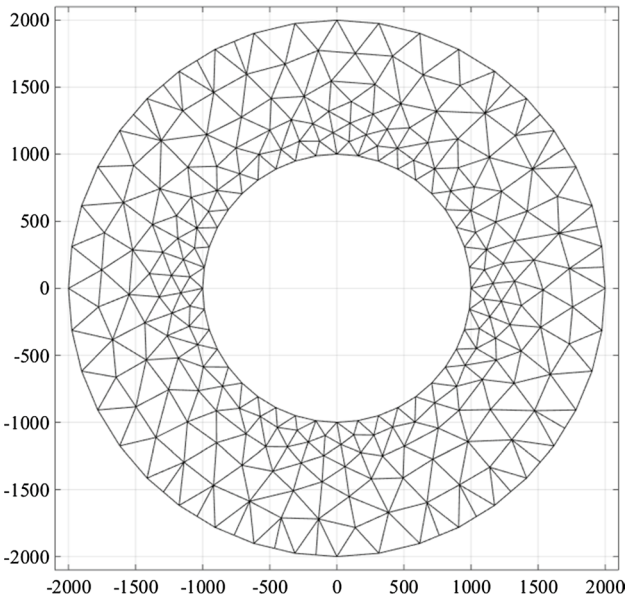

Fig. 8 Discretization of the expected elastoplastic region of 2-D example

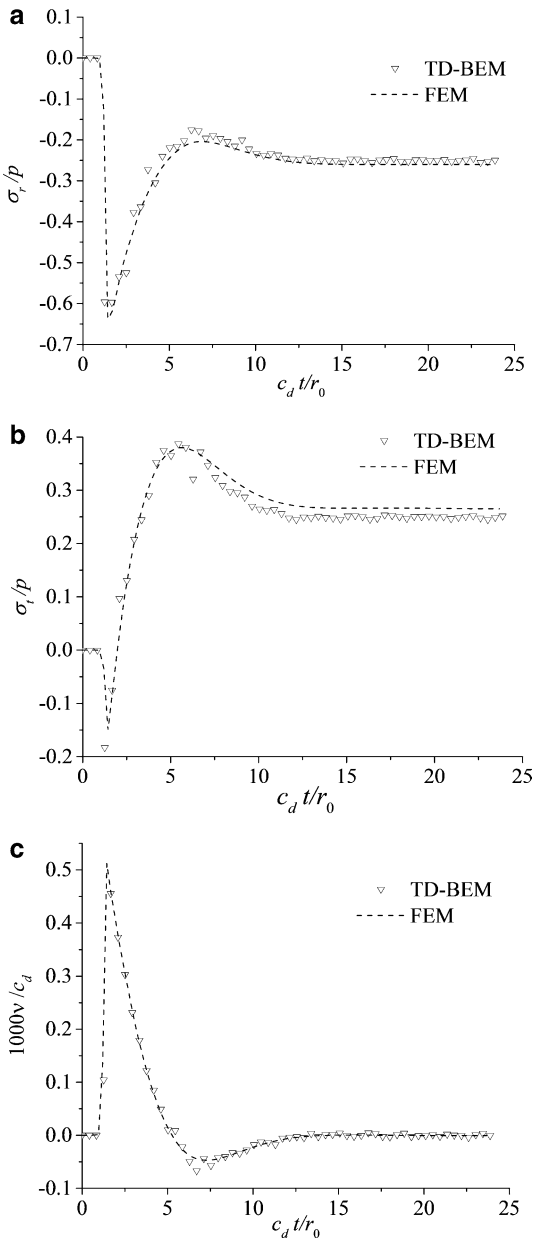

Fig. 9 Comparison between the results from TD-BEM and FEM for elastoplastic analysis ($r=2$ m) for **a** radial stress, **b** circumferential stress, and **c** velocity

3-nodded boundary elements, accordingly producing 40 boundary nodes and 231 domain nodes, shown in Fig. 8. The time step is 3.5×10^{-5} s. The FEM model is subscribed in Sect. 6.2.1.

The calculated waves at $r=2$ m from TD-BEM formulation for inelastic dynamic analysis are shown in Fig. 9(a–c) in terms of the radial stress, the circumferential stress and the velocity, respectively, where the results from FEM are also included. The corresponding waves at a farther radial distance from the center of the cavity, $r=8$ m, are shown in Fig. 10(a–c).

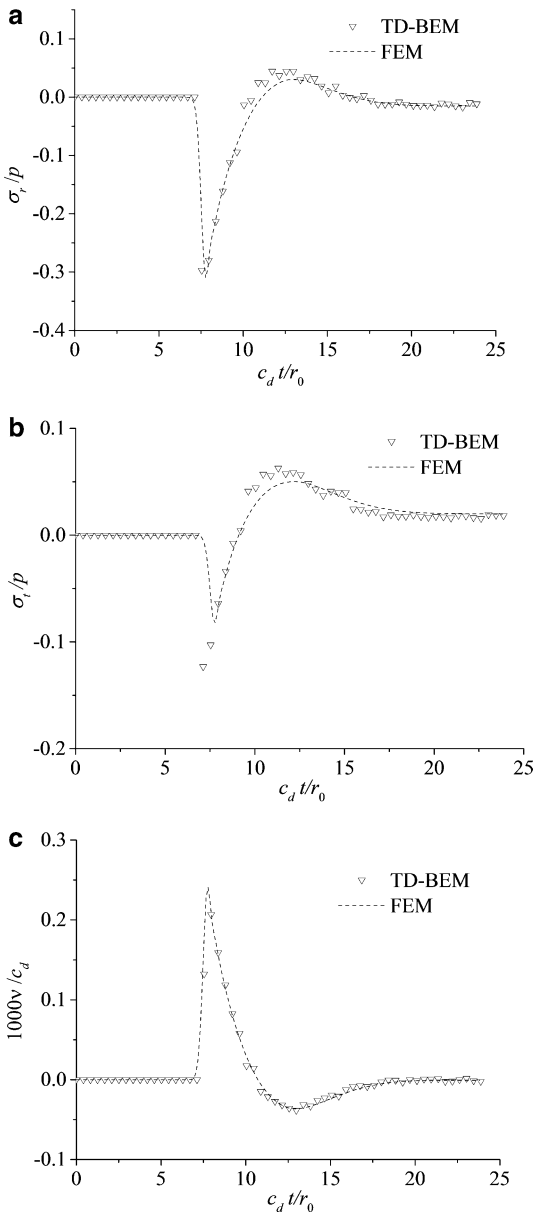

Fig. 10 Comparison between the results from TD-BEM and FEM for elastoplastic analysis ($r=8$ m) for **a** radial stress, **b** circumferential stress, and **c** velocity

From Figs. 9 and 10, by comparing the results both from the TD-BEM formulation for inelastic dynamic analysis and FEM, it can be seen that reasonably good agreement has been achieved for the points both close to and far away from the cavity boundary in the surrounding medium. By checking the peak value and the corresponding occurrence instant, a certain difference between results from TD-BEM formulation for inelastic analysis and FEM exists. The main reason for the difference might be that a large diameter plane domain is used to approximate the infinite domain in FEM model. Although the propagation range of the stress wave is completely included, a certain degree of difference still appears. By considering that the agreement with the objective analytical solution for the degenerated TD-BEM formulation for elastic analysis is better than for FEM, the peak values and the corresponding occurrence instant in Figs. 9 and 10 from TD-BEM formulation for inelastic analysis might be more convincing.

7 Conclusion

Based on the fundamental solution for traction and the relationship between stress and traction, the fundamental solution for stress is obtained. Upon the establishment of the fundamental solution for stress, by considering the law of volume elasticity, the equivalent stress boundary integral equation is established, where the virtual work in the third direction is considered.

Based on the equivalent stress fundamental solution, the boundary integral equations are proposed in this paper. The proposed boundary integral equations are applicable for plane strain problem and plane stress problem, by properly transforming the elastic parameters and adopting the corresponding fundamental solutions.

The whole formulation for transient dynamics based on 2-D TD-BEM frame is presented, where the numerical implementation and solution to the proposed boundary integral equations are briefed. The whole TD-BEM formulation for inelastic dynamic analysis can be degenerated to TD-BEM formulation for elastic dynamic analysis, by excluding the plastic integral term from the boundary integral equations.

The proposed TD-BEM formulation for inelastic dynamic analysis is validated from different viewpoints, for elastic and inelastic analysis, for one dimensional and 2-D geometries, and for finite and infinite domains.

Appendix A: Notations in the fundamental solutions

The parameters in the fundamental solutions in terms of displacement, traction and equivalent stress Eqs. (2), (3), (5) and (13), which are solely relevant with the spatial coordinate, are expressed as follows:

$$E_{ik} = \delta_{ik}, \tag{A1}$$

$$F_{ik} = \frac{\delta_{ik}}{r^2}, \tag{A2}$$

$$J_{ik} = -\frac{r_{,i}\, r_{,k}}{r^2}, \tag{A3}$$

$$A_{ik} = \mu\Big(2\varphi r_{,i}\, n_k + \delta_{ik}\frac{\partial r}{\partial n} + r_{,k}\, n_i\Big), \tag{A4}$$

$$B_{ik} = -\frac{2\mu}{r^3}\Big(\delta_{ik}\frac{\partial r}{\partial n} + r_{,i}\, n_k + r_{,k}\, n_i - 4\frac{\partial r}{\partial n} r_{,i}\, r_{,k}\Big), \tag{A5}$$

$$D_{ik} = -2\mu\Big(\varphi r_{,i}\, n_k + \frac{\partial r}{\partial n} r_{,i}\, r_{,k}\Big), \tag{A6}$$

$$A_{ikl} = \big(A_{ik}\big)_{n_w=\delta_{lw}} = \mu\big(2\varphi r_{,i}\, \delta_{kl} + \delta_{ik} r_{,l} + r_{,k}\, \delta_{il}\big), \tag{A7}$$

$$B_{ikl} = \big(B_{ik}\big)_{n_w=\delta_{lw}} = -\frac{2\mu}{r^3}\big(\delta_{ik} r_{,l} + r_{,i}\, \delta_{kl} + r_{,k}\, \delta_{il} - 4 r_{,i}\, r_{,k}\, r_{,l}\big), \tag{A8}$$

$$D_{ikl} = \big(D_{ik}\big)_{n_w=\delta_{lw}} = -2\mu\big(\varphi r_{,i}\, \delta_{kl} + r_{,i}\, r_{,k}\, r_{,l}\big), \tag{A9}$$

$$\overline{A}_{ikl} = A_{ikl} - \Delta A_{imm}\delta_{kl} = \mu\big[\delta_{ik} r_{,l} + r_{,k}\, \delta_{il}\big], \tag{A10}$$

$$\overline{B}_{ikl} = B_{ikl} = -\frac{2\mu}{r^3}\big(\delta_{ik} r_{,l} + r_{,i}\, \delta_{kl} + r_{,k}\, \delta_{il} - 4 r_{,i}\, r_{,k}\, r_{,l}\big). \tag{A11}$$

$$\overline{D}_{ikl} = D_{ikl} - \Delta D_{imm\delta kl} = -2\mu\big[r_{,i}\, r_{,k}\, r_{,l}\big]. \tag{A12}$$

The variables in the fundamental solutions in terms of displacement, traction and equivalent stress, Eqs. (2), (3), (5) and (13), which are relevant both with space and time, are expressed in the following equations

$$L_w = \big[c_w^2 (t-\tau)^2 - r^2\big]^{-\frac{1}{2}}, \tag{A13}$$

$$N_w = 2c_w^2 (t-\tau)^2 - r^2, \tag{A14}$$

$$H_w = H\big(M_w\big), \tag{A15}$$

$$M_w = c_w (t-\tau) - r. \tag{A16}$$

The following relationships exist among the aforementioned variables:

$$r = \big(r_w r_w\big)^{\frac{1}{2}}, \tag{A17}$$

$$r_w = x_w^Q - x_w^P, \tag{A18}$$

$$r_{,w} = \frac{\partial r}{\partial x_w^Q} = -\frac{\partial r}{\partial x_w^P} = \frac{r_w}{r}, \tag{A19}$$

$$\frac{\partial r_{,w}}{\partial x_v^Q} = -\frac{\partial r_{,w}}{\partial x_v^P} = \frac{\delta_{vw} - r_{,v}\, r_{,w}}{r}, \tag{A20}$$

$$n_v = \frac{\partial x_v}{\partial n}, \tag{A21}$$

$$\frac{\partial r}{\partial n} = r_{,w}\, n_w, \tag{A22}$$

$$n_w = n_v \delta_{vw}, \tag{A23}$$

$$r_{,w} = r_{,v}\, \delta_{vw}. \tag{A24}$$

The Lame constants and the relationship between the wave velocities are expressed as follows:

$$\mu = \frac{E}{2(1+\nu)}, \tag{A25}$$

$$\lambda = \frac{\nu E}{(1+\nu)(1-2\nu)}, \tag{A26}$$

$$c_s = \sqrt{\frac{\mu}{\rho}}, \tag{A27}$$

$$c_d = \sqrt{\frac{\lambda + 2\mu}{\rho}}, \tag{A28}$$

$$\varphi = \frac{\lambda}{2\mu} = \frac{c_d^2 - 2c_s^2}{2c_s^2}. \tag{A29}$$

Appendix B: Notations in stress boundary integral equation at interior points

D_w^p, S_w^u and Σ_w^ε in Eq. (19) respectively represent for the traction, displacement and plastic strain integral terms in stress boundary integral equation for elastoplastic dynamics, which are expressed by the following equations:

$$D_s^p = \int_\Gamma \left[\begin{array}{l} E_{ijk} \int_0^t c_s L_s p_k H_s \mathrm{d}\tau + E_{ijk}^0 \left| \int_0^t c_s \frac{\partial L_s}{\partial r} p_k H_s \mathrm{d}\tau \right| + F_{ijk} \int_0^t c_s L_s^{-1} p_k H_s \mathrm{d}\tau \\ + F_{ijk}^0 \left| \int_0^t c_s \frac{\partial \left(L_s^{-1}\right)}{\partial r} p_k H_s \mathrm{d}\tau \right| + J_{ijk} \int_0^t c_s L_s N_s p_k H_s \mathrm{d}\tau + J_{ijk}^0 \left| \int_0^t c_s \frac{\partial \left(L_s N_s\right)}{\partial r} p_k H_s \mathrm{d}\tau \right| \end{array} \right] \mathrm{d}\Gamma, \tag{B1}$$

$$D_d^p = \frac{c_s^2}{c_d^2} \int_\Gamma \left[\begin{array}{l} F_{ijk} \int_0^t c_d L_d^{-1} p_k H_d \mathrm{d}\tau + F_{ijk}^0 \left| \int_0^t c_d \frac{\partial \left(L_d^{-1}\right)}{\partial r} p_k H_d \mathrm{d}\tau \right| \\ + J_{ijk} \int_0^t c_d L_d N_d p_k H_d \mathrm{d}\tau + J_{ijk}^0 \left| \int_0^t c_d \frac{\partial \left(L_d N_d\right)}{\partial r} p_k H_d \mathrm{d}\tau \right| \end{array} \right] \mathrm{d}\Gamma, \tag{B2}$$

$$S_s^u = \int_\Gamma \left[\begin{array}{l} \left(A_{ijk} + D_{ijk}\right) \left| \int_0^t c_s r L_s^3 u_k H_s \mathrm{d}\tau \right| + \left(A_{ijk}^0 + D_{ijk}^0\right) \frac{\partial}{\partial r} \left| \int_0^t c_s r L_s^3 u_k H_s \mathrm{d}\tau \right| \\ + B_{ijk} \int_0^t c_s L_s N_s u_k H_s \mathrm{d}\tau + B_{ijk}^0 \left| \int_0^t c_s \frac{\partial \left(L_s N_s\right)}{\partial r} u_k H_s \mathrm{d}\tau \right| \end{array} \right] \mathrm{d}\Gamma, \tag{B3}$$

$$S_d^u = \frac{c_s^2}{c_d^2} \int_\Gamma \left[\begin{array}{l} B_{ijk} \int_0^t c_d L_d N_d u_k H_d \mathrm{d}\tau + B_{ijk}^0 \left| \int_0^t c_d \frac{\partial \left(L_d N_d\right)}{\partial r} u_k H_d \mathrm{d}\tau \right| \\ + D_{ijk} \left| \int_0^t c_d r L_d^3 u_k H_d \mathrm{d}\tau \right| + D_{ijk}^0 \frac{\partial}{\partial r} \left| \int_0^t c_d r L_d^3 u_k H_d \mathrm{d}\tau \right| \end{array} \right] \mathrm{d}\Gamma, \tag{B4}$$

$$\Sigma_s^\epsilon = \int_\Omega \left[\begin{array}{l} \left(A_{ijkl} + D_{ijkl}\right) \left| \int_0^t c_s r L_s^3 \varepsilon_{kl}^p H_s d\tau \right| + \left(A_{ijkl}^0 + D_{ijkl}^0\right) \frac{\partial}{\partial r} \left| \int_0^t c_s r L_s^3 \varepsilon_{kl}^p H_s d\tau \right| \\ + B_{ijkl} \int_0^t c_s L_s N_s \varepsilon_{kl}^p H_s d\tau + B_{ijkl}^0 \left| \int_0^t c_s \frac{\partial \left(L_s N_s\right)}{\partial r} \varepsilon_{kl}^p H_s d\tau \right| \end{array} \right] \mathrm{d}\Omega, \tag{B5}$$

$$\Sigma_d^\epsilon = \frac{c_s^2}{c_d^2} \int_\Omega \left[\begin{array}{l} B_{ijkl} \int_0^t c_d L_d N_d \varepsilon_{kl}^p H_d \mathrm{d}\tau + B_{ijkl}^0 \left| \int_0^t c_d \frac{\partial \left(L_d N_d\right)}{\partial r} \varepsilon_{kl}^p H_d \mathrm{d}\tau \right| \\ + D_{ijkl} \int_0^t c_d r L_d^3 \varepsilon_{kl}^p H_d \mathrm{d}\tau + D_{ijkl}^0 \frac{\partial}{\partial r} \left| \int_0^t c_d r L_d^3 \varepsilon_{kl}^p H_d \mathrm{d}\tau \right| \end{array} \right] \mathrm{d}\Omega. \tag{B6}$$

In the last two expressions, Ω_0 is the special integral domain, where the singular point (the source point) is scooped away from the overall integral domain Ω.

It is noted that, in the process of the solution of the kernel function in terms of strain influence coefficients, $\overline{\sigma}_{ijkl}^*$, the derivative of the equivalent stress fundamental solution with respect to the coordinates is involved, where the hyper

singularity arises. It has been shown that the concept of the finite part of an integral, Hadamard principle integral, is an efficient method to treat the hyper singularity. In order to manipulate the singularities in the process of the solution of the integral coefficients by means of Hadamard principle integral, the free term f_{ij}^{P} is introduced, by subtracting $\sigma_{ij}^{p}(P,t)$ from the independent integral at the singular point (the source point) as:

$$f_{ij}^{P} = -\frac{\mu}{4(1-\nu)}\Big[(1-4\nu)\delta_{ij}\varepsilon_{mm}^{p} + 2\varepsilon_{ij}^{p}\Big]. \tag{B7}$$

The coefficients in Eq. (19), which are solely relevant with the spatial coordinate are as follows:

$$E_{ijk} = 0, \tag{B8}$$

$$E_{ijk}^{0} = -\mu\big(\delta_{ik}r_{,j} + \delta_{jk}r_{,i} + 2\varphi\delta_{ij}r_{,k}\big), \tag{B9}$$

$$F_{ijk} = \frac{2\mu}{r^3}\big(\delta_{ik}r_{,j} + \delta_{jk}r_{,i} + 2\varphi\delta_{ij}r_{,k}\big), \tag{B10}$$

$$F_{ijk}^{0} = -\frac{\mu}{r^2}\big(\delta_{ik}r_{,j} + \delta_{jk}r_{,i} + 2\varphi\delta_{ij}r_{,k}\big), \tag{B11}$$

$$J_{ijk} = \frac{\mu}{r^3}\big(2\delta_{ij}r_{,k} + \delta_{jk}r_{,i} + \delta_{ik}r_{,j} - 8r_{,i}\,r_{,j}\,r_{,k} - 2\varphi\delta_{ij}r_{,k}\big), \tag{B12}$$

$$J_{ijk}^{0} = \frac{2\mu}{r^2}\big(r_{,i}\,r_{,j}\,r_{,k} + \varphi\delta_{ij}r_{,k}\big), \tag{B13}$$

$$\begin{aligned} A_{ijk} = \frac{\mu^2}{r}\Big[&-4\varphi n_k(\delta_{ij} - r_{,i}\,r_{,j}) + \frac{\partial r}{\partial n}(\delta_{ik}r_{,j} + \delta_{jk}r_{,i}) \\ &- 2(\delta_{ik}n_j + \delta_{jk}n_i) + r_{,i}\,r_{,k}\,n_j + r_{,j}\,r_{,k}\,n_i \\ &- 4\varphi\delta_{ij}(\varphi n_k + n_k - \frac{\partial r}{\partial n}r_{,k})\Big], \end{aligned} \tag{B14}$$

$$\begin{aligned} A_{ijk}^{0} = \mu^2\Big[&-4\varphi r_{,i}\,r_{,j}\,n_k - \frac{\partial r}{\partial n}(\delta_{ik}r_{,j} + \delta_{jk}r_{,i}) - r_{,i}\,r_{,k}\,n_j \\ &- r_{,j}\,r_{,k}\,n_i - 4\varphi\delta_{ij}(\varphi n_k + \frac{\partial r}{\partial n}r_{,k})\Big], \end{aligned} \tag{B15}$$

$$\begin{aligned} B_{ijk} = \frac{4\mu^2}{r^4}\Big[&4\frac{\partial r}{\partial n}(6r_{,i}\,r_{,j}\,r_{,k} - \delta_{ij}r_{,k} - \delta_{jk}r_{,i} - \delta_{ik}r_{,j}) \\ &+ (\delta_{ij}n_k + \delta_{jk}n_i + \delta_{ik}n_j) \\ &- 4(r_{,i}\,r_{,j}\,n_k + r_{,i}\,r_{,k}\,n_j + r_{,j}\,r_{,k}\,n_i)\Big], \end{aligned} \tag{B16}$$

$$\begin{aligned} B_{ijk}^{0} = \frac{2\mu^2}{r^3}\Big[&\frac{\partial r}{\partial n}(\delta_{jk}r_{,i} + \delta_{ik}r_{,j} - 8r_{,i}\,r_{,j}\,r_{,k}) \\ &+ 2r_{,i}\,r_{,j}\,n_k + r_{,i}\,r_{,k}\,n_j + r_{,j}\,r_{,k}\,n_i \\ &+ 2\varphi\delta_{ij}\Big(n_k - 2\frac{\partial r}{\partial n}r_{,k}\Big)\Big], \end{aligned} \tag{B17}$$

$$\begin{aligned} D_{ijk} = \frac{2\mu^2}{r}\Big[&2\varphi n_k(\delta_{ij} - r_{,i}\,r_{,j}) + r_{,i}\,r_{,k}\,n_j + r_{,j}\,r_{,k}\,n_i \\ &+ \frac{\partial r}{\partial n}(-6r_{,i}\,r_{,j}\,r_{,k} + 2\delta_{ij}r_{,k} + \delta_{jk}r_{,i} + \delta_{ik}r_{,j}) \\ &+ 2\varphi\delta_{ij}(\varphi n_k + \frac{\partial r}{\partial n}r_{,k})\Big], \end{aligned} \tag{B18}$$

$$\begin{aligned} D_{ijk}^{0} = 4\mu^2\Big[&\varphi n_k r_{,i}\,r_{,j} + \frac{\partial r}{\partial n}r_{,i}\,r_{,j}\,r_{,k} \\ &+ \varphi\delta_{ij}(\varphi n_k + \frac{\partial r}{\partial n}r_{,k})\Big], \end{aligned} \tag{B19}$$

$$\begin{aligned} A_{ijkl} = \frac{\mu^2}{r}\big[&\delta_{ik}r_{,j}\,r_{,l} + \delta_{jk}r_{,i}\,r_{,l} + \delta_{jl}r_{,i}\,r_{,k} + \delta_{il}r_{,j}\,r_{,k} \\ &- 2\big(\delta_{ik}\delta_{jl} + \delta_{jk}\delta_{il}\big) + 4\varphi\delta_{ij}r_{,k}\,r_{,l}\big], \end{aligned} \tag{B20}$$

$$\begin{aligned} A_{ijkl}^{0} = \mu^2[&-4\varphi\delta_{ij}r_{,l}\,r_{,k} - \delta_{ik}r_{,j}\,r_{,l} - \delta_{jk}r_{,i}\,r_{,l} \\ &- r_{,i}\,r_{,k}\,\delta_{jl} - r_{,j}\,r_{,k}\,\delta_{il}], \end{aligned} \tag{B21}$$

$$\begin{aligned} B_{ijkl} = \frac{4\mu^2}{r^4}[&(\delta_{ij}\delta_{kl} + \delta_{jk}\delta_{il} + \delta_{ik}\delta_{jl}) + 24r_{,i}\,r_{,j}\,r_{,k}\,r_{,l} \\ &- 4(\delta_{ij}r_{,k}\,r_{,l} + \delta_{jk}r_{,i}\,r_{,l} + \delta_{ik}r_{,j}\,r_{,l} \\ &+ \delta_{kl}r_{,i}\,r_{,j} + \delta_{jl}r_{,i}\,r_{,k} + \delta_{il}r_{,j}\,r_{,k})], \end{aligned} \tag{B22}$$

$$\begin{aligned} B_{ijkl}^{0} = \frac{2\mu^2}{r^3}[&\delta_{jk}r_{,i}\,r_{,l} + \delta_{ik}r_{,j}\,r_{,l} + 2\delta_{kl}r_{,i}\,r_{,j} + \delta_{jl}r_{,i}\,r_{,k} \\ &+ \delta_{il}r_{,j}\,r_{,k} - 8r_{,i}\,r_{,j}\,r_{,k}\,r_{,l} + 2\varphi\delta_{ij}(\delta_{kl} - 2r_{,k}\,r_{,l})], \end{aligned} \tag{B23}$$

$$\begin{aligned} D_{ijkl} = \frac{2\mu^2}{r}[&2(\varphi+1)\delta_{ij}r_{,k}\,r_{,l} + \delta_{jl}r_{,i}\,r_{,k} + \delta_{il}r_{,j}\,r_{,k} \\ &+ (\delta_{jk}r_{,i}\,r_{,l} + \delta_{ik}r_{,j}\,r_{,l} - 6r_{,i}\,r_{,j}\,r_{,k}\,r_{,l})], \end{aligned} \tag{B24}$$

$$D_{ijkl}^{0} = 4\mu^2\big[\varphi\delta_{ij}r_{,k}\,r_{,l} + r_{,i}\,r_{,j}\,r_{,k}\,r_{,l}\big]. \tag{B25}$$

Acknowledgement The authors would like to acknowledge the financial support provided by Hebei Education Department (Grant QN2020135), the National Key R&D Program of China (Grants 2019YFC1511105 and 2019YFC1511104), and the National Natural Science Foundation of China (Grant 51778193).

References

1. Providakis, C.P., Beskos, D.E.: Dynamic analysis of plates by boundary elements. Appl. Mech. Rev. **52**, 213–236 (1999)
2. Hatzigeorgiou, G.D., Beskos, D.E.: Dynamic inelastic structural analysis by the BEM: A review. Eng. Anal. Bound. Elem. **35**, 159–169 (2011)
3. Beskos, D.E.: Boundary element methods in dynamic analysis: Part II (1986–1996). Appl. Mech. Rev. **50**, 149–197 (1997)
4. Brebbia, C.A.: The birth of the boundary element method from conception to application. Eng. Anal. Bound. Elem. **77**, iii–x (2017)
5. Soares, D.: Dynamic anlysis of elastoplastic models considering combined formulations of the time-domain boundary element method. Eng. Anal. Bound. Elem. **55**, 28–39 (2015)
6. Zheng, B.J., Gao, X.W., Zhang, C.: Radial integration BEM for vibration analysis of two- and three-dimensional elasticity structures. Appl. Math. Comput. **277**, 111–126 (2016)
7. Carrer, J.A.M., Telles, J.C.F.: A boundary element formulation to solve transient dynamic elastoplastic problems. Comput. Struct. **45**, 707–713 (1992)
8. Eshraghi, I., Dag, S.: Domain-boundary element method for elastodynamics of functionally graded Timoshenko beams. Comput. Struct. **195**, 113–125 (2018)
9. Carrer, J.A.M., Corrêa, R.M., Mansur, W.J., et al.: Dynamic analysis of continuous beams by the boundary element method. Eng. Anal. Bound. Elem. **104**, 80–93 (2019)
10. Kontoni, D.P.N., Beskos, D.E.: Transient dynamic elastoplastic analysis by the dual reciprocity BEM. Eng. Anal. Bound. Elem. **12**, 1–16 (1993)
11. Hamzehei-Javaran, S., Khaji, N.: Complex Fourier element shape functions for analysis of 2D static and transient dynamic problems using dual reciprocity boundary element method. Eng. Anal. Bound. Elem. **95**, 222–237 (2018)
12. Soares, R.A., Palermo, L., Wrobel, L.C.: Application of the dual reciprocity method for the buckling analysis of plates with shear deformation. Eng. Anal. Bound. Elem. **106**, 427–439 (2019)
13. Dominguez, J.: Boundary Elements in Dynamics. Computational Mechanics Publications and Elsevier Applied Science, Southampton and London (1993)
14. Banerjee, P.K., Raveendra, S.T.: Advanced boundary element analysis of two- and three-dimensional problems of elasto-plasticity. Int. J. Num. Meth. Engng. **23**, 985–1002 (1986)
15. Israil, A.S.M., Banerjee, P.K.: Advanced development of boundary element method for two-dimensional dynamic elasto-plasticity. Int. J. Solids. Struct. **29**, 1433–1451 (1992)
16. Scuciato, R.F., Carrer, J.A.M., Mansur, W.J.: The time-dependent boundary element method formulation applied to dynamic analysis of Euler-Bernoulli beams: the linear θ method. Eng. Anal. Bound. Elem. **79**, 98–109 (2017)
17. Soares, D., Carrer, J.A.M., Mansur, W.J.: Non-linear elastodynamic analysis by the BEM: An approach based on the iterative coupling of the D-BEM and TD-BEM formulations. Eng. Anal. Bound. Elem. **29**, 761–774 (2005)
18. Yu, G.Y., Mansur, W.J., Carrer, J.A.M., et al.: A more stable scheme for BEM/FEM coupling applied to two-dimensional elastodynamics. Comput. Struct. **79**, 811–823 (2001)
19. Elleithy, W.M., Tanaka, M.: Interface relaxation algorithms for BEM-BEM coupling and FEM-BEM coupling. Comput. Meth. Appl. Mech. Eng. **192**, 2977–2992 (2003)
20. Telles, J.C.F., Brebbia, C.A.: On the application of the boundary element method to plasticity. Appl. Math. Model. **3**, 466–470 (1979)
21. Brebbia, C.A., Telles, J.C.F., Wrobel, L.C., et al.: Boundary Element Techniques: Theory and Applications in Engineering. Springer-Verlag, New York (1984)
22. Brebbia, C.A.: Boundary Element Method for Engineers. Pentech Press, Plymouth and London (1978)
23. Telles, J.C.F., Carrer, J.A.M., Mansur, W.J.: Transient dynamic elastoplastic analysis by the time-domain BEM formulation. Eng. Anal. Bound. Elem. **23**, 479–486 (1999)
24. Hadamard, J.: Lectures on Cauchy's Problem in Linear Partial Differential Equations. Courier Dover Publications, Dover (2003)
25. Simpson, R.N., Bordas, S.P.A., Trevelyan, J., et al.: A two-dimensional isogeometric boundary element method for elastostatic analysis. Comput. Methods Appl. Mech. Engrg. **209–212**, 87–100 (2012)
26. Kuhn, G., Möhrmann, W.: Boundary element method in elastostatics: theory and applications. Appl. Math. Model. **7**, 97–105 (1983)
27. Lei, W.D., Ji, D.F., Li, H.J., et al.: On an analytical method to solve singular integrals both in space and time for 2-D elastodynamics by TD-BEM. Appl. Math. Model. **39**, 6307–6318 (2015)
28. Xie, G.Z., Zhong, Y.D., Zhou, F.L., et al.: Singularity cancellation method for time-domain boundary element formulation of elastodynamics: A direct approach. Appl. Math. Model. **80**, 647–667 (2020)
29. Mansur, W.J.: A time-stepping technique to solve wave propagation problems using the boundary element method. [Ph.D. Thesis], University of Southampton, Southampton (1983).
30. Lei, W.D., Li, H.J., Qin, X.F., et al.: Dynamics-based analytical solutions to singular integrals for elastodynamics by time domain boundary element method. Appl. Math. Model. **56**, 612–625 (2018)
31. Peng, H.F., Yang, K., Cui, M., et al.: Radial integration boundary element method for solving two-dimensional unsteady convection-diffusion problem. Eng. Anal. Bound. Elem. **102**, 39–50 (2019)
32. Marrero, M., Dominguez, J.: Numerical behavior of time domain BEM for three-dimensional transient elastodynamic problem. Eng. Anal. Bound. Elem. **27**(1), 39–48 (2003)
33. Schanz, M., Antes, H.: Application of 'operational quadrature methods' in time domain boundary element methods. Meccanica **32**(3), 179–186 (1997)
34. Li, Y., Zhang, J., Zhong, Y., et al.: Transient elastodynamic analysis with a combination of convolution quadrature method and pseudo-initial condition method. Eng. Comput. **36**(1), 334–355 (2019)
35. Carrer, J.A.M., Mansur, W.J.: Stress and velocity in 2D transient elastodynamic analysis by the boundary element method. Eng. Anal. Bound. Elem. **23**, 233–245 (1999)
36. Ji, D.F., Lei, W.D., Li, H.J.: Corner treatment by assigning dual tractions to every node for elastodynamics in TD-BEM. Appl. Math. Comput. **284**, 125–135 (2016)
37. Eringen, A.C., Suhubi, E.S.: Elastodynamics, Linear Theory 2. Academic Press, New York (1975)
38. Chou, P.C., Koenig, H.A.: A unified approach to cylindrical and spherical elastic waves by method of characteristics. J. Appl. Mech. **33**, 159 (1966)